Robust Sensor Fault Estimation for LPV systems: Application to Quadrotor UAV

Eslam Abouselima, Dalil Ichalal, Saïd Mammar

Robust Sensor Fault Estimation for LPV systems: Application to Quadrotor UAV

Eslam Abouselima, Dalil Ichalal and Said Mammar

***Abstract*— This work is dedicated to handling the problem of quadrotor sensors fault diagnosis where the vehicle model is expressed in an LPV framework and accompanied by a robust self-scheduled LPV controller which minimizes the quadratic performance $\mathscr{H}_\infty$ norm. Afterward, a new observer scheme including a virtual residual signal beside an auxiliary output is introduced to achieve quadrotor sensor fault estimation and isolation. Through the synthesis of such an observer gains assignment, some structural conditions are discussed to guarantee exact or at least asymptotic convergence of the residual to the fault followed by an enhanced $\mathscr{H}_-/\mathscr{H}_\infty$ approach when the decoupling conditions are not satisfied. F inally, t he efficiency of the developed approach in fault estimation is demonstrated by applying it in simulation on a quadrotor UAV subjected to sensor faults.**

I. INTRODUCTION

Nowadays autonomous systems have gained a huge share of scientific r esearch t hanks t o t he i ncreasing technology evolution. Such a rapid expansion of the word automation has triggered a great concern for another critically important branch of automatic control which is Fault Tolerant Control (FTC). FTC systems are defined in [1] as the control systems that possess the ability to accommodate component failures automatically, this can be performed through two steps: Fault Detection and Diagnosis (FDD), and control reconfiguration.

Unmanned Aerial Vehicles (UAVs) take part as one of the most applications that need to be provided with FTC algorithms to enhance their reliability and robustness against system malfunction. Among these UAVs there exists the quadrotor which is very practical for various applications like surveillance and risk management thanks to its small volume and the advantage of vertical take-off and landing (VTOL). Usually, a quadrotor is equipped with lightweight, low-cost sensors like IMU for orientation and ultrasonic for altitude, and despite their acceptable performance in nominal conditions, they are vulnerable to sensor faults see [2]. According to [3], around 15% of UAVs failures result from the navigation system malfunction which urges this work to investigate the design of a sensor FDD unit for a quadrotor.

The mathematical model of the vehicle dynamics is derived based on Newton-Euler formulation in a similar way to the work presented in [4]. Indeed, the constructed system model has to be precise yet simple to convey further real-time control law application which is achieved by the Linear Parameter Varying (LPV) representation. An LPV system is defined b y [5] a s a t ype o f l inear t ime-varying system whose state space matrices are functions of bounded time-varying parameters. The robust self-scheduled LPV control law proposed in [6] was such an efficient method for feedback controller design, so it has been enhanced adopted by recent works as [7] and [8] for quadrotor control. In this work, a quadratic observer-based feedback controller is utilized to achieve reference tracking while being robust to the undesired inputs.

The methodology followed in [9] shows how important an FDD unit is for establishing an effective sensor FTC algorithm where the controller reconfiguration is based on the residual signal obtained after system diagnosis. Among several techniques for fault diagnosis, there exists the model based approach where $\mathscr{H}_\infty$ strategies and eigenstructure assignment are used for generating robust residual signals see [10]. Based on the $\mathscr{H}_-/\mathscr{H}_\infty$ technique an observer is introduced in [11] for sensor fault detection that minimizes exogenous disturbance effect while maximizing the fault effect on the residual signal. Such technique has shown great potential compared to the stochastic approach using Kalman filter see [12], however, the regularity condition [13] needed for quadratic constraints feasibility was satisfied by introducing a virtual perturbation term for the outputs. The progress of noisy signal estimation approaches like [14] and [15] has inspired the work of [16] to develop a more convenient solution for the regularity constraint depending on output signal derivatives and its associated relative degree.

Such advancements have been benefited in our previous work [17] which introduced a new residual generator scheme containing a virtual residual signal accompanied by a weighting matrix that defines the residual signals type. By analyzing the resulting error dynamics, it is proven that there exist some structural conditions that, if satisfied, enable the residual signal to converge exactly or at least asymptotically to the fault. Furthermore, an enhanced $\mathscr{H}_-/\mathscr{H}_\infty$ is proposed for fault diagnosis if these decoupling conditions are not satisfied. As a result, this paper represents an expansion for this work which can be deployed for sensor fault diagnosis by means of output integration [18] where the sensor faults are remodeled to be affecting system states. Thus, the main contributions of this paper are listed as follows:

- achieving sensor fault estimation using an auxiliary output which avoids the fault signal derivatives estimation while satisfying the regularity condition.
- accurate representation of the effect of exogenous disturbances on the system output.
- synthesizing the residual generator gains assignment for exact and asymptotic residual to fault convergence.

All the authors are with IBISC Laboratory, University of Evry, Paris-Saclay, Evry, 91000, France. Emails: (eslam.abouselima, dalil.ichalal, said.mammar)@ibisc.univ-evry.fr

- validating the obtained results by simulating a quadrotor LPV model subjected to sensors faults and exogenous disturbances.

II. Quadrotor LPV Model and Robust Control

A. Nonlinear model

A quadrotor vehicle has four actuators and is commonly constructed in a cross configuration as illustrated in figure 1. One popular method to model such system dynamics is the Newton-Euler formula assuming that the quadrotor is a symmetric rigid structure whose body axes origin is located at the center of gravity.

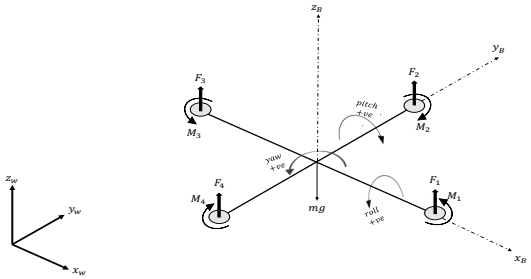

Fig. 1: Quadrotor schematic with motors forces and moments

Consider the following state vector containing the system position and orientation states:

$$X_s(t) = [x \quad y \quad z \quad \phi \quad \theta \quad \psi \quad \dot{x} \quad \dot{y} \quad \dot{z} \quad \dot{\phi} \quad \dot{\theta} \quad \dot{\psi}]^T \quad (1)$$

while the control input vector representing the motor forces and moments described by:

$$u(t) = [u_z, u_\phi, u_\theta, u_\psi, \Omega_r]^T \quad (2)$$

where u_ϕ, u_θ, u_ψ are the control inputs corresponding to the rotations around y, x, z axes, respectively, while u_z represents the total thrust along z axis, and Ω_r is the residual angular speed. The relation between the control input (2) and the state vector (1) is derived using Newton's second law for linear and angular motion with the aid of Euler angles and Euler rates matrices to transfer the forces, moments, and inertia properties from the inertial frame to the body-fixed frame resulting in the nonlinear model given by (3) (Notice that the derivation is omitted due to space limitation, however, one can refer to [4] where a full illustration is developed).

$$\dot{X}_s(t) = \begin{bmatrix} \dot{x} \\ \dot{y} \\ \dot{z} \\ \dot{\phi} \\ \dot{\theta} \\ \dot{\psi} \\ (\cos\phi\cos\psi\sin\theta + \sin\phi\sin\psi)\frac{u_z}{m} \\ (-\cos\psi\sin\phi + \cos\phi\sin\theta\sin\psi)\frac{u_z}{m} \\ \cos\theta\cos\phi\frac{u_z}{m} - g \\ \frac{\dot{\theta}\dot{\psi}(I_{yy}-I_{zz}) + \dot{\theta}J_r\Omega_r + u_\phi}{I_{xx}} \\ \frac{\dot{\phi}\dot{\psi}(I_{zz}-I_{xx}) - \dot{\phi}J_r\Omega_r + u_\theta}{I_{yy}} \\ \frac{\dot{\phi}\dot{\theta}(I_{xx}-I_{yy}) + u_\psi}{I_{zz}} \end{bmatrix} \quad (3)$$

where I_{xx}, I_{yy}, I_{zz} are the body moments of inertia, while the terms J_r, l, g represent the propeller inertia, arm length, and gravity acceleration, respectively.

B. LPV framework preliminaries

Consider a general nonlinear system given by

$$\begin{cases} \dot{x}(t) = f(x(t), u(t)) \\ y(t) = h(x(t), u(t)) \end{cases} \quad (4)$$

By a proper choice of the nonlinear terms that need to be expressed as varying parameters besides adding the sensor faults and exogenous disturbance effect, the resulting LPV system can be represented by

$$\begin{cases} \dot{x}(t) = A(\rho(t))x(t) + B(\rho(t))u(t) + E(\rho(t))d(t) \\ y(t) = C(\rho(t))x(t) + F(\rho(t))f(t) \end{cases} \quad (5)$$

where $x(t) \in \mathbb{R}^n, y(t) \in \mathbb{R}^{n_y}$, $u(t) \in \mathbb{R}^{n_u}, d(t) \in \mathbb{R}^{n_d}$, and $f(t) \in \mathbb{R}^{n_f}$ are the state, output, input, disturbance, and fault vectors, respectively, while their corresponding state space matrices are $A(.), B(.), E(.), C(.), F(.)$ depending on the vector of varying parameters $\rho^T(t) = \big(\rho_1(t), ..., \rho_{n_\rho}(t)\big)$.

Assumption 1: Through the analysis of the LPV system, the time-varying parameters are assumed to have known bounds on the magnitude and rate of change, hence their values are smoothly evolving within these limits along some specific linear trajectories.

Given that a varying parameter is called $\rho_i(t)$, then the bounds on its magnitude and time derivatives can be described by

$$\rho_i^{min} \leq \rho_i(t) \leq \rho_i^{max} \quad (6)$$

$$\rho_i^{(j)min} \leq \rho_i^{(j)}(t) \leq \rho_i^{(j)max} \quad (7)$$

where $\rho_i^{(j)min}$ and $\rho_i^{(j)max}$, $i = 1, ..., n_\rho$ define the minimum and maximum values of the j^{th} time derivative of the parameter $\rho_i^{(j)}(t)$.

Based on the results of assumption 1, the vectors of the varying parameters and their time derivatives belong to hyperrectangle compact sets illustrated in [19] within which they vary along smooth continuous trajectories according to time (Lipschitz condition). The LPV systems can be categorized by different classes according to the dependency of the model matrices on the varying parameters. In this work, the LPV model (5) is an affine polytopic system containing n_ρ parameters which are evolving through a convex polytope having a number of vertices $w = 2^{n_\rho}$. Thus, the resulting varying parameters matrices can be represented by the following convex form

$$\mathscr{M}(\rho(t)) = \sum_{k=1}^{w} \nu_k(\rho(t))\mathscr{M}_k \quad (8)$$

such that $\mathscr{M}(.) \in \{A(.), B(.), E(.), F(.), C(.)\}$, hence, at each instant of time, the value of the state space matrices depends on the interpolation between the varying parameters ultimate values described by the weighting functions ν_k, $k = 1, ..., w$ which satisfy the following convex property:

$$\begin{cases} 0 \leq \nu_k(\rho(t)) \leq 1, \quad \forall t, k = 1, \ldots, w \\ \sum_{k=1}^{w} \nu_k(\rho(t)) = 1 \end{cases} \quad (9)$$

It follows that the derivatives of the varying parameters matrices which are important for constructing the auxiliary output as discussed later are given by

$$\frac{d\mathscr{M}(\rho(t))}{dt} = \sum_{k=1}^{w} \nu_k(\dot{\rho}(t))\mathscr{M}_k \tag{10}$$

Assumption 2: Based on the convexity property of the LPV system (5), the conditions applied to the LPV model (such as the controllability and observability) hold for all possible values of $\rho(t)$ if and only if they hold at the LPV model vertices following the results of [6].

Assumption 3: Throughout this work, the output relative degree to faults and disturbances denoted λ_f and λ_d discussed in [17] is assumed to be uniform such that they are independent of the variation of the parameters and their successive time derivatives.

C. Quadrotor quasi-LPV model

Commonly, the quadrotor control is constructed in a cascaded scheme where the inner loop including the fast dynamics attitude states gets the command from the outer loop representing the slower dynamics position states. So in this work, the dynamics of the attitude and altitude states are investigated, and thus the state vector is reduced to

$$x(t) = [\quad \phi \quad \theta \quad \psi \quad z \quad \dot{\phi} \quad \dot{\theta} \quad \dot{\psi} \quad \dot{z}]^T \tag{11}$$

After eliminating the position dynamics from equation (3) and by assuming that the system executes its motion through small perturbations around the hovering point, hence the trigonometric functions can be approximated by $\sin\theta \approx \theta$, $\cos\theta \approx 1$. Then by choosing the terms $\dot{\theta}$ and $\dot{\phi}$ as the varying parameters, the resulting model conveys a quasi-LPV representation where the varying parameters are the system states. Thus, the vector of the varying parameters is $\rho(t) = [\dot{\theta}, \dot{\phi}]$ and the system can be described by the polytopic form in (5) with the following time-varying matrices:

$$A(\rho(t)) = \begin{bmatrix} 0_{4\times4} & I_{4\times4} \\ 0_{4\times4} & A_\sigma \end{bmatrix}, B(\rho(t)) = \begin{bmatrix} 0_{4\times5} \\ B_\sigma \end{bmatrix}, C(\rho(t)) = \begin{bmatrix} I_{8\times8} \end{bmatrix} \tag{12}$$

$$A_\sigma = \begin{bmatrix} 0 & 0 & \frac{\dot{\theta}(I_{yy}-I_{zz})}{I_{xx}} & 0 \\ 0 & 0 & \frac{\dot{\phi}(I_{zz}-I_{xx})}{I_{yy}} & 0 \\ \frac{\dot{\theta}(I_{xx}-I_{yy})}{I_{zz}} & 0 & 0 & 0 \\ 0 & 0 & 0 & 0 \end{bmatrix}, \; B_\sigma = \begin{bmatrix} 0 & \frac{1}{I_{xx}} & 0 & 0 & \frac{\dot{\theta}J_r}{I_{xx}} \\ 0 & 0 & \frac{1}{I_{yy}} & 0 & \frac{-\dot{\phi}J_r}{I_{yy}} \\ 0 & 0 & 0 & \frac{1}{I_{zz}} & 0 \\ \frac{1}{m} & 0 & 0 & 0 & 0 \end{bmatrix} \tag{13}$$

The exogenous disturbances to be included in the model depend on the environmental conditions within which the drone will be operating. So in this work, two of the common outdoor quadrotor disturbances listed in table I are included, namely gust wind, and gravity acceleration which are described mathematically by

$$d(t) = \begin{bmatrix} d_1(t), d_2(t), d_3(t) \end{bmatrix} \tag{14}$$

where $d_1(t)$ and $d_2(t)$ are representing gust wind force in y and x directions, respectively, in addition to $d_3(t) = g$ describing the effect of the drone weight which allows the controller to adapt to the varying payload.

$$E(\rho(t)) = \begin{bmatrix} E_1 \\ E_2 \end{bmatrix}, E_1 = \begin{bmatrix} 0.1 & 0 & 0 \\ 0 & 0.1 & 0 \\ 0 & 0 & 0 \\ 0 & 0 & 0 \end{bmatrix}, E_2 = \begin{bmatrix} 1 & 0 & 0 \\ 0 & 1 & 0 \\ 0 & 0 & 0 \\ 0 & 0 & -1 \end{bmatrix} \tag{15}$$

TABLE I: Sensor faults and external disturbances

faults	disturbances
bias	gust wind
drift	acceleration of gravity
freezing	payload
loss of accuracy	terrain induced wind
calibration error	propeller vortex

Finally, $F(\rho(t))$ represents the impact of sensor faults $f(t)$ on the output $y(t)$, thus its value depends on the sensors used and their common faults. Some typical aircraft sensor faults given in table I are investigated earlier in [1] and since this work is dedicated to attitude and altitude fault diagnosis, two main sensors are considered IMU and Ultrasonic.

Regarding the IMU, the readings of angular rates $(\dot{\phi}, \dot{\theta}, \dot{\psi})$ are obtained from the gyroscope which can be affected by the structural vibrations and loose fixations resulting in loss of accuracy. Furthermore, the orientation angles (ϕ, θ, ψ) are calculated by integrating the angular rates so such measurements are vulnerable to error accumulation (drift). Concerning the ultrasonic sensor, the major problem is freezing due to range limitations and speed of data acquisition. A convenient way to represent all the aforementioned kinds of faults on the measurement is to have two matrices as follows:

$$F_m = \begin{bmatrix} I_{4\times4} & 0_{4\times4} \end{bmatrix}, \quad F_r = \begin{bmatrix} 0_{4\times4} & I_{4\times4} \end{bmatrix} \tag{16}$$

Such that the vector f(t) contains the sensors parametric faults, then according to which sensor to be examined there are two possibilities:

- $F(\rho(t)) = F_m$, for altitude and orientation faults.
- $F(\rho(t)) = F_r$, for ascending and angular rates faults.

This is an efficient way to estimate the exact value of a sensor fault while avoiding the coupled states effect, for example, a residual in the direction of ϕ is not affected by a fault of the angular velocity $\dot{\phi}$ and so on.

D. Observer-based feedback control

The proposed control law is similar to that utilized in our previous work [17] where an additive state $\dot{\tilde{z}} = -\kappa\tilde{z} + z$ is included to produce an integral action in the direction of altitude z-axis. This method is appealing as it enables the designed control law to adapt to the quadrotor weight if there is an extra payload according to the tuned value of the constant parameter κ. After examining the controllability of the pair $(A(\rho(t)), B(\rho(t)))$, the following observer-based feedback control law is introduced in a polytopic form to achieve reference tracking

$$u(t) = -K(\rho(t))\hat{x}(t) + N(\rho(t))\eta(t) \tag{17}$$

where $\hat{x}$ and $\eta(t)$ are the estimated state and the reference input, respectively, while the feedback gain matrix $K(.)$ and the DC gain inverse matrix $N(.)$ are parameter varying matrices which conform with the polytopic form given by equation (8). The following inequalities (18) and (19) are used to deduce the values of the feedback gain matrices at the polytope vertices $K_j, j \in \{1, \dots w\}$

$$(A_k - B_k K_j)^T \Psi + \Psi(A_k - B_k K_j) + 2\zeta_c \Psi < 0 \tag{18}$$

$$\begin{pmatrix} (A_k - B_k K_j)^T \Psi + \Psi(A_k - B_k K_j) & \Psi B_k & {C_k}^T \\ {B_k}^T \Psi & -{\gamma_c}^2 I & {D_k}^T \\ C_k & D_k & -I \end{pmatrix} < 0 \tag{19}$$

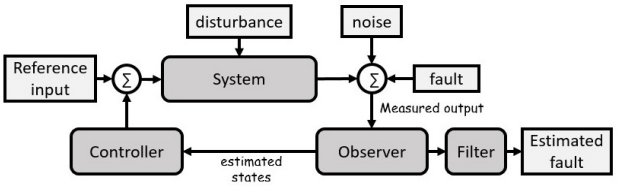

Fig. 2: Fault diagnosis schematic

By a simple change of variables the inequalities (18) and (19) are transformed into LMIs to be solved using YALMIP optimization tool [20] aiming to reach the minimum value of γ_c while preserving the matrix Ψ as positive definite. The inequality (18) corresponds to Lyapunov quadratic stability and guarantees the accuracy of the closed loop system time response. While the inequality (19) represents the Bounded Real Lemmma (BRL) which ensures the exogenous signals effect to be less than the quadratic $\mathscr{H}_\infty$ performance level γ_c following the results of [6]. The LPV controller can be regarded as a self-scheduled control law due to its dependence on the-varying parameters which are the system states in our quasi-LPV model. Finally, to guarantee precise reference tracking, the DC gain inverse $N(\rho(t))$ obtained from equation (20) is introduced such that the steady-state error that can arise due to a time-varying input is eliminated.

$$N(\rho(t)) = -\Big(C(\rho(t))\big[A(\rho(t)) - B(\rho(t))K(\rho(t))\big]^{-1}B(\rho(t))\Big)^{\dagger} \tag{20}$$

where $\Lambda^{\dagger}$ represents the pseudo-inverse of the matrix Λ

III. Sensor Fault Estimation

In this work, we are seeking a robust residual generator that is able to develop a reliable sensor fault estimation during the presence of exogenous disturbances and measurement noise see figure 2. By investigating the literature two main challenging problems are found, namely regularity condition satisfaction and exact residual to fault convergence, in this section a solution for each one will be presented. In order to apply the method discussed in [17] for sensor fault diagnosis, the system (5) can be rewritten for simplicity as follows

$$\begin{cases} \dot{x}(t) = A_\rho x(t) + B_\rho u(t) + E_\rho d(t) \\ y(t) = C_\rho x(t) + F_\rho f(t) \end{cases} \tag{21}$$

by defining a new state $\varepsilon(t) = \int_0^t y(\tau)\,d\tau, \varepsilon(t) \in \mathbb{R}^{n_y}$ such that

$$\dot{\varepsilon}(t) = C_\rho x(t) + F_\rho f(t) \tag{22}$$

Then the following augmented system can be constructed

$$\begin{cases} \dot{x}_a(t) = \bar{A}_\rho x_a(t) + \bar{B}_\rho u(t) + \bar{E}_\rho d(t) + \bar{F}_\rho f(t) \\ y_a(t) = \bar{C}_\rho x_a(t) \end{cases} \tag{23}$$

where $x_a(t) = \begin{bmatrix} x(t) \\ \varepsilon(t) \end{bmatrix}$, $\bar{A}_\rho = \begin{bmatrix} A_\rho & 0 \\ C_\rho & 0 \end{bmatrix}$, $\bar{B}_\rho = \begin{bmatrix} B_\rho \\ 0 \end{bmatrix}$, $\bar{E}_\rho = \begin{bmatrix} E_\rho \\ 0 \end{bmatrix}$, $\bar{F}_\rho = \begin{bmatrix} 0 \\ F_\rho \end{bmatrix}$, $\bar{C}_\rho = \begin{bmatrix} 0 & I_{n_y} \end{bmatrix}$, represent the augmented system matrices with appropriate dimensions. This procedure is deployed in [18] to design an observer with an additive integral action while the observability of the pair $(\bar{A}_\rho, \bar{C}_\rho)$ is guaranteed under the following assumption.

Assumption 4: For every complex number s with non-negative real part:

$$rank\begin{bmatrix} sI_n - A_\rho & E_\rho \\ C_\rho & 0 \end{bmatrix} = n + rank(E_\rho) \tag{24}$$

A. auxiliary output

As mentioned before, to guarantee a feasible solution for the problem of $\mathscr{H}_\infty$ norm minimization, the regularity assumption should be satisfied. The common way adopted in the literature is to introduce a term modeling the disturbance effect on the output, however, a promising method is proposed in [16] based on an extended output of the system containing the output and its successive time derivatives named the auxiliary output $\tilde{y}(t)$. Such an output provides a more realistic impact of the disturbances, but obviously, it depends on signal differentiation which can amplify the measurement noise effect. Fortunately, the recent algorithms developed for estimating the high order time derivatives of a signal such as high-gain differentiators [14] and numerical differentiators [15] are able to provide robust signal differentiation that is less sensitive to the noises affecting the signal. Consider $\tilde{y}(t)$ is given by

$$\tilde{y}(t) = \begin{bmatrix} y_a(t) \\ \dot{y}_a(t) \end{bmatrix} = \begin{bmatrix} \bar{C}_\rho x_a(t) \\ \bar{C}_\rho \dot{x}_a(t) \end{bmatrix} \tag{25}$$

or in another form

$$\tilde{y}(t) = C_{\tilde{\rho}} x_a(t) + B_{\tilde{\rho}} u(t) + R_{\tilde{\rho}} f(t) + D_{\tilde{\rho}} d(t) \tag{26}$$

where $C_{\tilde{\rho}} = \begin{bmatrix} \bar{C}_\rho \\ \bar{C}_\rho \bar{A}_\rho \end{bmatrix}$, $B_{\tilde{\rho}} = \begin{bmatrix} 0 \\ \bar{C}_\rho \bar{B}_\rho \end{bmatrix}$, $R_{\tilde{\rho}} = \begin{bmatrix} 0 \\ \bar{C}_\rho \bar{F}_\rho \end{bmatrix}$, $D_{\tilde{\rho}} = \begin{bmatrix} 0 \\ \bar{C}_\rho \bar{E}_\rho \end{bmatrix}$ are system matrices with appropriate dimensions and $\tilde{\rho}(t)$ represents the vector of the parameters $\rho(t)$ and their time derivatives.

Since sensor faults are considered, then their effect appears in the 1^{st} output time derivative (relative degree of fault to output is $\lambda_f = 1$). Fortunately regarding the quadrotor model (12) to (16), the disturbance affect the 1^{st} output time derivative thus the regularity condition is satisfied in the auxiliary output (25). Note if another system has a relative degree from disturbance to output $\lambda_d > 1$, then it is necessary to estimate input and fault derivatives, such an issue can be interesting for future work.

B. virtual residual

As this work pursue a robust observer that is able to perform fault diagnosis (detection, estimation, and isolation), the same residual generator produced in our previous work [17] is utilized taking the following form

$$\begin{cases} \dot{\hat{x}}_a(t) = \bar{A}_\rho \hat{x}_a(t) + \bar{B}_\rho u(t) + L_{1\tilde{\rho}}\left(y_a(t) - \hat{y}_a(t)\right) + L_{2\tilde{\rho}}\left(\tilde{y}(t) - \hat{\tilde{y}}(t)\right) \\ \hat{y}_a(t) = \bar{C}_\rho \hat{x}_a(t) \\ \hat{\tilde{y}}(t) = C_{\tilde{\rho}} \hat{x}_a(t) + B_{\tilde{\rho}} u(t) \\ r(t) = M_{\tilde{\rho}}\left(\tilde{y}(t) - \hat{\tilde{y}}(t)\right) \end{cases} \tag{27}$$

In addition, we introduce the reference residual vector $r_r(t) = Qf(t)$, where Q is a the fault weighting matrix that defines the type of the obtained residual signals as illustrated in [17]. In this way, if the residual generator objective is to perform fault detection along a specific direction, the weighting matrix Q is chosen as a vector along this direction. In our case, we aim to perform fault estimation so the weighting matrix is chosen to be $Q = I_{n_f}$ where I_{n_f} is the identity matrix of dimensions $n_f \times n_f$. Furthermore, a virtual residual signal defined by $r_e(t) = r(t) - r_r(t) = r(t) - Qf(t)$

is added aiming to minimize its magnitude such that the residual $r(t)$ converges to the fault $f(t)$.

IV. Residual Generator Gains Assignment

This section aims to assign the values of the gain matrices $L_{1\bar{\rho}}$, $L_{2\bar{\rho}}$ and $M_{\bar{\rho}}$ to ensure robust fault diagnosis where two procedures for exact and asymptotic residual to fault convergence are discussed followed by the worst case $\mathscr{H}_-/\mathscr{H}_\infty$ approach if non of the decoupling conditions are satisfied. So consider the system (23) and (26) accompanied with the residual generator (27), given the state error $e(t) = x_a(t) - \hat{x}_a(t)$ the resulting error dynamics will be

$$\begin{cases} \dot{e}(t) = \left(\bar{A}_\rho - L_{1\bar{\rho}}\bar{C}_\rho - L_{2\bar{\rho}}C_{\bar{\rho}}\right)e + \left(\bar{F}_\rho - L_{2\bar{\rho}}R_{\bar{\rho}}\right)f(t) \\ \quad + \left(\bar{E}_\rho - L_{2\bar{\rho}}D_{\bar{\rho}}\right)d(t) \\ r_e(t) = M_{\bar{\rho}}C_{\bar{\rho}}e(t) + \left(M_{\bar{\rho}}R_{\bar{\rho}} - Q\right)f(t) + M_{\bar{\rho}}D_{\bar{\rho}}d(t) \end{cases} \tag{28}$$

which can be rewritten in the following form

$$\begin{cases} \dot{e}(t) = A_{e\rho}e(t) + E_{f\rho}f(t) + E_{d\rho}d(t) \\ r_e(t) = C_{e\rho}e(t) + F_{f\rho}f(t) + F_{d\rho}d(t) \end{cases} \tag{29}$$

A. Exact convergence

It has been proven in [17] that if the system satisfies the following condition

$$rank\left(\begin{bmatrix} C_{\bar{\rho}} & R_{\bar{\rho}} & D_{\bar{\rho}} \\ 0 & Q & 0 \end{bmatrix}\right) = rank\left(\begin{bmatrix} C_{\bar{\rho}} & R_{\bar{\rho}} & D_{\bar{\rho}} \end{bmatrix}\right), \forall \bar{\rho}(t) \in \bar{\Phi} \tag{30}$$

then, the matrix $M_{\bar{\rho}}$ can be chosen as

$$M_{\bar{\rho}} = \begin{bmatrix} 0 & Q & 0 \end{bmatrix}\begin{bmatrix} C_{\bar{\rho}} & R_{\bar{\rho}} & D_{\bar{\rho}} \end{bmatrix}^\dagger \tag{31}$$

which will guarantee exact convergence of the residual signal to the reference residual resulting in $r_e(t) = 0$ or in other words $r(t) = Qf(t)$.

It is evident from the results of this approach that the residual signal is independent of the error dynamics, hence the matrix $L_{1\bar{\rho}}$ can be fixed to zeros. However, for practical cases where the output derivatives can't be guaranteed to be exact, the gain $L_{1\bar{\rho}}$ can be calculated using pole placement such that the residual generator can perform state estimation also. Nevertheless, if the system doesn't convey the condition (30), then asymptotic residual to fault convergence can be maintained by assigning the observer gain matrices according to the following technique.

B. Asymptotic convergence

Again based on the results obtained in [17], if the following conditions hold

$$rank\left(R_{\bar{\rho}}\right) = n_f, \quad rank\left(\begin{bmatrix} \bar{F}_\rho \\ R_{\bar{\rho}} \end{bmatrix}\right) = rank\left(\bar{F}_\rho\right) \tag{32}$$

then, the matrices $M_{\bar{\rho}}$ and $L_{2\bar{\rho}}$ can be chosen as

$$\begin{cases} M_{\bar{\rho}} = QR_{\bar{\rho}}^\dagger \\ L_{2\bar{\rho}} = \bar{F}_\rho R_{\bar{\rho}}^\dagger \end{cases} \tag{33}$$

In that manner, the fault effect is decoupled from the error dynamics (28) and under the observability of the pair $(\bar{A}_\rho - L_{2\bar{\rho}}C_{\bar{\rho}}, \bar{C}_\rho)$, the gain matrix $L_{1\bar{\rho}}$ can be calculated in a way that minimizes the effect of the disturbances on the error dynamics such that

$$\|r(t) - Qf(t)\|_2 < \gamma\|d(t)\|_2 \tag{34}$$

which results in asymptotic convergence of the residual signal to the fault

$$\lim_{t\to+\infty} r(t) = Qf(t) \tag{35}$$

Here arises the importance of the gain $L_{1\bar{\rho}}$ which offers an additional degree of freedom to assign the observer poles position such that it can perform fault estimation in the nominal case even if the value of the other two gains $M_{\bar{\rho}}$ and $L_{2\bar{\rho}}$ are fixed. The gain $L_{1\bar{\rho}}$ can be computed to minimize the quadratic $\mathscr{H}_\infty$ performance level γ by solving the Bounded Real Lemma (BRL) illustrated in the next section where a general solution based on the $\mathscr{H}_-/\mathscr{H}_\infty$ technique is proposed as our last option for observer gains assignment when the system doesn't convey any of the aforementioned decoupling conditions.

C. Alternative $\mathscr{H}_-/\mathscr{H}_\infty$ technique

Recall the error dynamics given by (29) which is affected by the existence of faults and disturbances simultaneously. The target of this approach is to assign the residual generator gain matrices $M_{\bar{\rho}}, L_{1\bar{\rho}}, L_{2\bar{\rho}}$ in a way that ensures the maximum sensitivity of the residual to the fault $||T_{rf}||_- \geq \beta$ besides the minimum influence of the exogenous disturbance $||T_{rd}||_\infty \leq \gamma$ while preserving a fast time response for precise fault estimation. These three objectives are settled by solving the following inequalities (a detailed derivation can be found in [12])

$$\begin{pmatrix} {A_{e\rho}}^T P + PA_{e\rho} & PE_{f_\rho} & -{C_{e\rho}}^T \\ {E_{f_\rho}}^T P & -\beta^2 I & -{F_{f_\rho}}^T \\ -C_{e\rho} & -F_{f_\rho} & -I \end{pmatrix} < 0 \tag{36}$$

$$\begin{pmatrix} {A_{e\rho}}^T P + PA_{e\rho} & PE_{d\rho} & {C_{e\rho}}^T \\ {E_{d\rho}}^T P & -\gamma^2 I & {F_{d\rho}}^T \\ C_{e\rho} & F_{d\rho} & -I \end{pmatrix} < 0 \tag{37}$$

$${A_{e\rho}}^T P + PA_{e\rho} + 2\zeta_o P < 0 \tag{38}$$

where ζ_o is a positive scalar to be chosen to determine the observer time constant. The three inequalities (37), (36), (38) can be transformed into LMIs by introducing the variables $V_{1\rho} = PL_{1\bar{\rho}}$ and $V_{2\rho} = PL_{2\bar{\rho}}$. Then, the resulting optimization problem is solved for a symmetric positive definite matrix P with an objective function $max(\beta^2 - \gamma^2)$ using semi-definite programming solver called 'SEDUMI' see [20].

V. Simulation Results

In order to reveal the effectiveness of the proposed approach in sensor fault estimation, it is applied to the quadrotor quasi-LPV model detailed in section II.C having the inertia properties given by [21] in simulation using Matlab-Simulink. As previously mentioned through calculating the auxiliary output $\tilde{y}(t)$, the faults and disturbances appear in the 1^{st} time derivative of the system output. Hence, the relative degree the relative degrees from the faults and disturbances to the output are equal $\lambda_f = \lambda_d = 1$, however, it is not satisfying the condition of exact convergence (30). Afterward, while checking the asymptotic convergence conditions, the system is found to comply with the conditions (32) but the resulting

pair $(\bar{A}_\rho - L_{2\bar{\rho}}C_{\bar{\rho}}, \bar{C}_\rho)$ is not observable. So the $\mathscr{H}_-/\mathscr{H}_\infty$ approach presented in section IV.C is used to obtain the gain matrices $L_{1\bar{\rho}}, L_{2\bar{\rho}}$, and $M_{\bar{\rho}}$. Note: the discussed theorems have shown great potential for fault estimation while applied for some academic examples having different system models but they are omitted due to space limitation.

Before proceeding to the residual generator optimization problem solution, the upper and lower limits of the angular velocities as varying parameters are chosen from the nonlinear model simulation performed in our previous work [12] to be $\rho(t) \in [-0.5, 0.5]\ rad/s$. For the controller design, the following constants are chosen $\zeta_c = 2,\ \kappa = 5$ to add an integral action along z-direction beside keeping the closed-loop system poles on the left hand side of $\sigma = -2$ in the s-plane. Concerning the residual generator design, the constant $\zeta_o = 4$ is introduced to ensure fast time response and after solving the convex optimization problem, the resulting values of β^2 and γ^2 are equal to 1.24 and 1.0924, respectively. To give a better understanding of the simulation environment, the initial condition of the state vector in (11) is $x(0) = 0$ except for $z(0) = 1$ and its estimated value is given by $\hat{x}(0) = 0.1$. While the included disturbances are low-frequency sinusoidal gust wind given by

$$\begin{cases} d_1(t) = 0.5\sin 0.8t & t > 20s \\ d_1(t) = 0.5\cos 0.8t & t > 20s \end{cases} \tag{39}$$

Finally, the measured attitude, altitude, angular rates, and rate of ascending are subjected to white Gaussian noises $n_s(t) \in [-0.03, 0.03]$ and $n_v(t) \in [-.06, .06]$ having a sample time of $0.03, 0.01\ s$, respectively. The results demonstrated by figure 3 shows the residual generator response in fault free case that proves the ability of the proposed algorithm to attenuate the noise effect while providing the controller with smoothly estimated states to attain reference tracking. Furthermore, the effect of both initial conditions and wind disturbances on the observer response is of a negligible order of magnitude compared to the case where a real fault does exist.

To demonstrate the potential of the proposed $\mathscr{H}_-/\mathscr{H}_\infty$ technique in fault estimation the states of the system are subjected to the faults given by

$$f_s(t) = \begin{cases} 2^\circ & t > 10\ s \\ (2 + 0.4t)^\circ & t > 10\ s \\ 5^\circ & 10 \le t \le 15\ s \\ -\hat{z} + \hat{z}(T_f) & 8 \le t \le 12\ s \end{cases} \tag{40}$$

The fault signal (40) represents a bias in the reading of (ϕ), a drift of (θ) (which as mentioned before likely to happen as the IMU integrates the $(\dot{\theta})$ measurement provided by the gyroscope), and a sudden abrupt change of (ψ). In addition, the altitude z is subjected to freezing fault given by f_{s4} where $T_f = 8s$ is the start time, such fault is common for ultrasonic sensors due to their measuring range limits. The results shown in figure 4 demonstrate the capabilities of the residual generator in fault detection and estimation of simultaneous different faults affecting the states measurements despite of the exogenous disturbances existence.

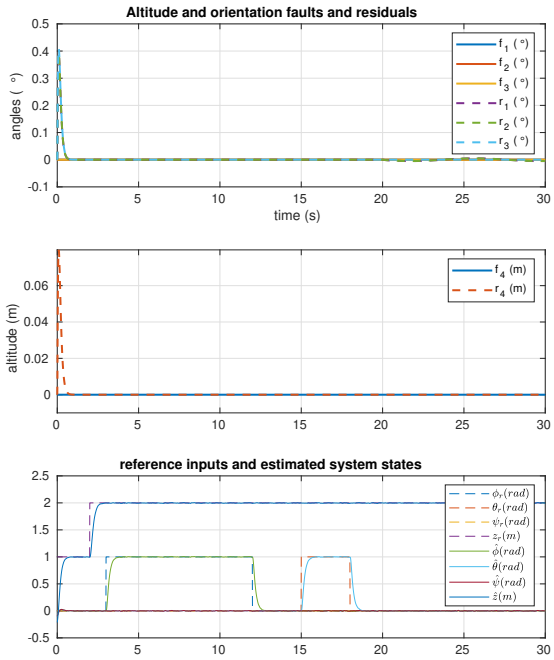

Fig. 3: Fault free case

$$f_r(t) = \begin{cases} (5\sin 0.8t + 2\cos 2.4t)^\circ/s & t > 10\ s \\ (4\sin 0.5t + 3\cos t)^\circ/s & t > 10\ s \\ 10^\circ/s & 5 \le t \le 7\ s \\ 0.2m/s & 10 \le t \le 12\ s \end{cases} \tag{41}$$

Furthermore, by considering $F(\rho(t)) = F_r$ given in (16), the climbing and angular rates are subjected to the sensors faults given by (41). Such faults represent time varying gyroscope malfunction of $\dot{\phi}$ and $\dot{\theta}$ while $\dot{\psi}$ and $\dot{z}$ are affected by sudden finite time changes.

Again the results shown in figure 5 illustrate great potential of the proposed algorithm for the gyroscope time-varying and abrupt faults estimation. In addition, although the gravity effect is modeled as a disturbance on the system, it doesn't prohibit asymptotic convergence of the residual signal to the fault. The results obtained here are very promising for further sensor fault-tolerant control design as the residual generator is able to identify the amount and location of fault precisely.

VI. Conclusion

In this paper, a newly developed model-based observer scheme is deployed as a residual generator which is provided with a virtual residual signal to perform sensor fault estimation. An additive integral action is introduced to promote the ability of the system to model the effect of the disturbances on the measurements, in a way that increases its robustness. Moreover, augmenting the system with an integral action helps to avoid the problem resulting from the control input and the fault differentiation while computing the auxiliary output. The auxiliary output is introduced based on the output relative degree to satisfy the regularity condition needed to ensure the feasibility of the quadratic $\mathscr{H}_\infty$ performance constraints. Through synthesizing the residual gains assignment, two notions are investigated, namely exact and asymptotic

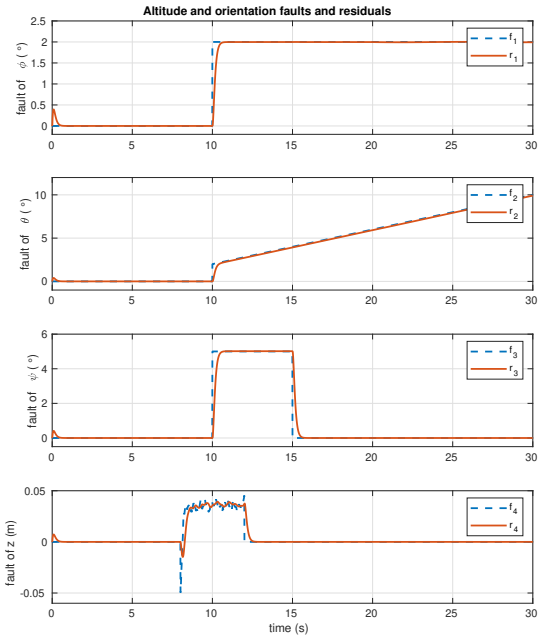

Fig. 4: Faults vs residuals for system states

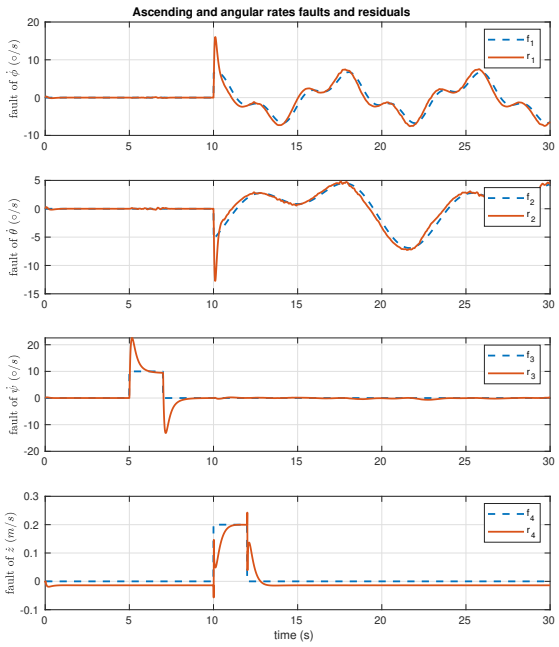

Fig. 5: Faults vs residuals for states derivatives

residual to fault convergence depending on the mathematical model properties. If the system is not satisfying any of the decoupling conditions, then the min/max technique based on the $\mathscr{H}_-/\mathscr{H}_\infty$ norms is used for computing the observer gain matrices. Finally, the proposed approach is tested by means of simulation of the quadrotor quasi-LPV model accompanied by a robust observer-based feedback control law. The adequate simulation results in fault estimation exhibit great potential of the proposed residual generator to be further used in active sensor fault-tolerant control.

REFERENCES

[1] Halim Alwi, Christopher Edwards, and Chee Pin Tan. *Fault detection and fault-tolerant control using sliding modes*. Springer Science & Business Media, 2011.

[2] Remus C Avram, Xiaodong Zhang, and Jonathan Muse. Quadrotor sensor fault diagnosis with experimental results. *Journal of Intelligent & Robotic Systems*, 86(1):115–137, 2017.

[3] Enrico Petritoli, Fabio Leccese, and Lorenzo Ciani. Reliability and maintenance analysis of unmanned aerial vehicles. *Sensors*, 18(9):3171, 2018.

[4] Carlos Trapiello, Vicenç Puig, and Bernardo Morcego. Position-heading quadrotor control using lpv techniques. *IET Control Theory & Applications*, 13(6):783–794, 2019.

[5] Damiano Rotondo, Fatiha Nejjari, Abel Torren, and Vicenc Puig. Fault tolerant control design for polytopic uncertain lpv systems: Application to a quadrotor. In *2013 Conference on Control and Fault-Tolerant Systems (SysTol)*, pages 643–648. IEEE, 2013.

[6] Pierre Apkarian, Pascal Gahinet, and Greg Becker. Self-scheduled $\mathscr{H}_\infty$ control of linear parameter-varying systems: a design example. *Automatica*, 31(9):1251–1261, 1995.

[7] Iman Sadeghzadeh, Abbas Chamseddine, Didier Theilliol, and Youmin Zhang. Linear parameter varying control synthesis: State feedback versus $\mathscr{H}_\infty$ technique with application to quadrotor ua v. In *2014 International Conference on Unmanned Aircraft Systems (ICUAS)*, pages 1099–1104. IEEE, 2014.

[8] Samarathunga LMD Rangajeeva and James F Whidborne. Linear parameter varying control of a quadrotor. In *2011 6th International Conference on Industrial and Information Systems*, pages 483–488. IEEE, 2011.

[9] Dalil Ichalal, Benoît Marx, José Ragot, Said Mammar, and Didier Maquin. Sensor fault tolerant control of nonlinear takagi–sugeno systems. application to vehicle lateral dynamics. *International Journal of Robust and Nonlinear Control*, 26(7):1376–1394, 2016.

[10] Julien Marzat, Hélène Piet-Lahanier, Frédéric Damongeot, and Eric Walter. Model-based fault diagnosis for aerospace systems: a survey. *Proceedings of the Institution of Mechanical Engineers, Part G: Journal of aerospace engineering*, 226(10):1329–1360, 2012.

[11] FR López Estrada, Jean Christophe Ponsart, Didier Theilliol, and Carlos-Manuel Astorga-Zaragoza. Robust $\mathscr{H}_-/\mathscr{H}_\infty$ fault detection observer design for descriptor-lpv systems with unmeasurable gain scheduling functions. *International Journal of Control*, 88(11):2380–2391, 2015.

[12] Eslam Abouselima, Dalil Ichalal, and Saïd Mammar. Quadrotor control and actuator fault detection: Lqg versus robust $\mathscr{H}_-/\mathscr{H}_\infty$ observer. In *2019 4th Conference on Control and Fault Tolerant Systems (SysTol)*, pages 86–91. IEEE, 2019.

[13] Amr M Pertew, Horacio J Marquez, and Qing Zhao. $\mathscr{H}_\infty$ observer design for lipschitz nonlinear systems. *IEEE Transactions on Automatic Control*, 51(7):1211–1216, 2006.

[14] Salim Ibrir. Online exact differentiation and notion of asymptotic algebraic observers. *IEEE transactions on Automatic control*, 48(11):2055–2060, 2003.

[15] Michel Fliess, Cédric Join, and Hebertt Sira-Ramirez. Non-linear estimation is easy. *International Journal of Modelling, Identification and Control*, 4(1):12–27, 2008.

[16] D Ichalal, B Marx, D Maquin, and J Ragot. Actuator fault diagnosis: $\mathscr{H}_\infty$ framework with relative degree notion. *IFAC-PapersOnLine*, 49(5):321–326, 2016.

[17] Eslam Abouselima, Dalil Ichalal, and Said Mammar. Robust actuator fault diagnosis for lpv systems: Application to quadrotor. In *2021 American Control Conference (ACC)*, pages 4938–4945. IEEE, 2021.

[18] Jian Zhang, Akshya Kumar Swain, and Sing Kiong Nguang. *Robust observer-based fault diagnosis for nonlinear systems using MATLAB®*. Springer, 2016.

[19] Dalil Ichalal and Saïd Mammar. On unknown input observers for lpv systems. *IEEE Transactions on Industrial Electronics*, 62(9):5870–5880, 2015.

[20] J. Löfberg. Yalmip : A toolbox for modeling and optimization in matlab. In *In Proceedings of the CACSD Conference*, Taipei, Taiwan, 2004.

[21] Kostas Alexis, George Nikolakopoulos, Yannis Koveos, and Antonios Tzes. Switching model predictive control for a quadrotor helicopter under severe environmental flight conditions. *IFAC Proceedings Volumes*, 44(1):11913–11918, 2011.